Fermi National Accelerator Laboratory

FERMILAB-Conf-94/393

The 1994 Fermilab Fixed Target Program

Janet Conrad

Fermi National Accelerator Laboratory
P.O. Box 500, Batavia, Illinois 60510

November 1994

Presented at the *XXII Summer Institute on Particle Physics Topical Conference Particle Physics, Astrophysics and Cosmology,* Stanford Linear Accelerator Center, Stanford, California, August 8-19, 1994

Disclaimer

THE 1994 FERMILAB FIXED TARGET PROGRAM

Janet Conrad
Columbia University
New York, New York 10027

ABSTRACT

The Fermilab Fixed Target Program covers measurements of hadron structure, precision tests of the Standard Model, studies of heavy quark production, determination of polarization and magnetic moments and searches for new phenomena. Highlights of the results of the last year are discussed here.

1 Introduction

This paper highlights the results of the Fermilab Fixed Target Program that were announced between October, 1993 and October, 1994. These results are drawn from 18 experiments that took data in the 1985, 1987 and 1990/91 fixed target running periods. The program is quite diverse and many interesting results have been published recently,[1] so it is not possible to review all of the new measurements. The plans for the next Fermilab fixed target run, scheduled to begin in 1996, also are included in this article.

For this discussion, the Fermilab Fixed Target Program is divided into 5 major topics: Hadron Structure, Precision Electroweak Measurements, Heavy Quark Production, Polarization and Magnetic Moments, and Searches for New Phenomena. However, it should be noted that most experiments span several subtopics. Also, measurements within each subtopic often affect the results in other subtopics. For example, parton distributions from hadron structure measurements are used in the studies of heavy quark production.

Due to restrictions on space, this discussion must presuppose familarity with many concepts. References 2-6 provide useful reviews of the ideas associated with each topic below. Reference 7, *The Fermilab Workbook*, describes the ongoing program at FNAL and each experiment.

2 Hadron Structure Experiments

Nucleon structure studies are interesting as universal, fundamental measurements, as tests of QCD and as constraints on the parton distributions. The data from muon and neutrino experiments at FNAL can be compared as a test of the universality of the structure functions. New data from muon scattering experiments extend the measurement of F_2 into previously unexplored kinematic regions. New precision measurements of structure functions provide an opportunity to test QCD evolution and extract the QCD parameter Λ, which sets the scale of the strong interaction. In the kinematic regions where the structure of the nucleon can be interpreted in terms of quarks, certain processes provide high sensitivity to each distribution. Global analyses which include all of the FNAL fixed target data provide the best parameterizations of the individual parton distributions.

The hadron structure experiments at Fermilab use a variety of beams and

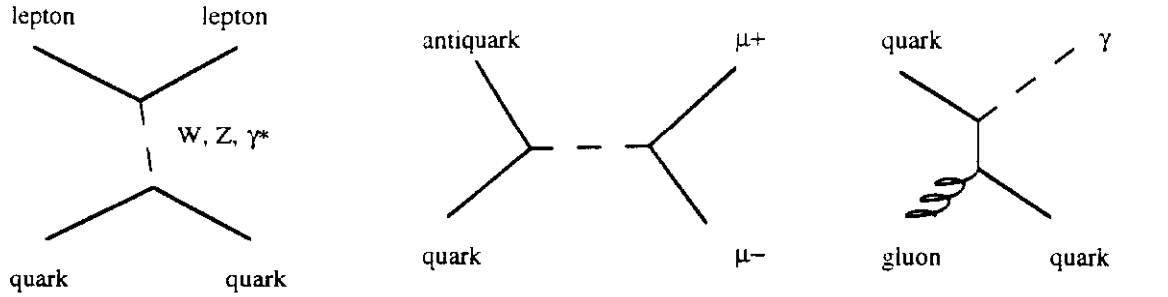

Figure 1: Examples of processes used to study hadron structure.

detectors. This section will cover new measurements from the deep inelastic neutrino and muon scattering experiments (E744/770 and E665, respectively), the Drell-Yan experiment (E772/789), and the direct photon production experiment (E706). Figure 1 shows examples of each of these processes.

2.1 Neutrino and Muon Measurements of F_2

The parity-conserving structure function F_2 is measured by deep inelastic lepton scattering experiments. In the deep inelastic regime, F_2 can be defined as:

$$F_2 = \sum_{i=u,\bar{u},\ldots} {e_i}^2 x q_i(x, Q^2) \tag{1}$$

where i is the quark type, e_i is the charge associated with the interaction, and q_i is the probability of finding a quark of type i with fractional momentum x in the nucleon. In the case of muon scattering, the coupling is electromagnetic, hence the definition of F_2 includes the quark charges squared. In neutrino scattering, the corresponding "weak charge" is unity.

Over the past decade many precision muon and neutrino experiments have been performed at CERN and at FNAL. Below, the new results on F_2 from the CCFR (E744/770) neutrino experiment at FNAL are compared to both the older results from the NMC muon experiment at CERN and to the preliminary results from the E665 muon scattering experiment at FNAL.

As a result of the difference in charge coupling (e_i) between the electromagnetic and weak interactions, a conversion must be applied in order to compare muon

and neutrino experiments. To lowest order, the correction is:

$$F_2^\mu = \frac{5}{18} F_2^\nu \left[1 - \frac{3(s+\bar{s})}{5(q+\bar{q})} \right]. \tag{2}$$

The strange sea (s, $\bar{s}$) appears explicitly in this equation. This can be precisely measured by charged-current neutrino scattering from strange quarks. This process has the unique signature of producing two muons of opposite sign, one from the scattered lepton and the other from the semileptonic decay of the produced charm. The CCFR next-to-leading-order measurement of the strange sea extracted from these events is used to make the corrections in this discussion.[8]

Nuclear effects must also be considered when comparing muon and neutrino measurements of F_2. Neutrino scattering experiments typically use high-density nuclear targets because the neutrino cross section is very small. The CCFR results were obtained with an iron target (bound nucleons). The electromagnetic cross section is reasonably large and so muon experiments typically use hydrogen and deuterium (free and loosely-bound nucleons, respectively). The difference in F_2 between bound nucleons and free nucleons has been studied in muon experiments. The corrections used below are from NMC.[9]

Figure 2 compares the F_2 measured by CCFR[10] to the measurements from NMC.[11] The corrections for charge coupling and nuclear effects have been applied to the muon data. F_2 is shown as a function of the squared four-momentum transfer, Q^2, for a wide range of x. From these plots one can see that there is good agreement between the measurements for $x > 0.1$; however, there is disagreement at low x. The disagreement increases with decreasing x.

One cause for the disagreement may be the nuclear correction. This correction assumes that effects in scattering from bound nucleon targets are the same for muons and neutrinos in the low x ("shadowing") region. However, if shadowing effects are caused by fluctuations of the intermediate virtual boson to mesons, then one might expect differences. The vector-meson-dominance model ascribes the cause of shadowing to fluctuations of the vector boson into mesons leading to strong interactions near the "surface" of the nucleon. In the case of muon scattering the photon can fluctuate only into vector mesons, while for neutrinos the W has an axial as well as a vector component. It should also be noted that E665 at FNAL has recently presented preliminary results which indicate that smaller nuclear corrections may be needed,[12] making the neutrino and muon F_2 measurements more compatible.

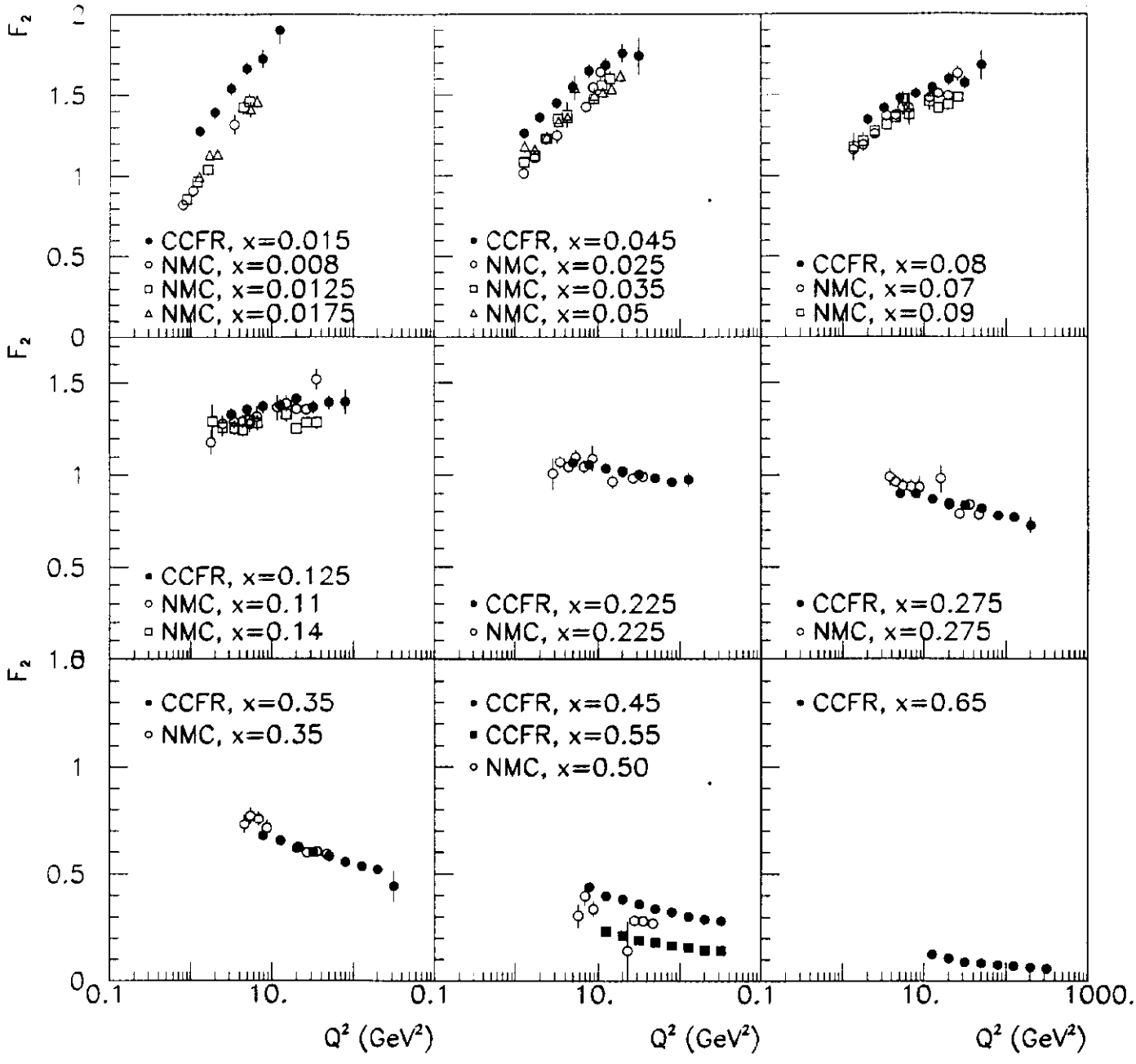

Figure 2: Comparison of the CCFR (ν) measurement of F_2 to the NMC (μ) result. Corrections for definition of F_2 and for nuclear effects (see text) were applied to the NMC data to permit comparison.

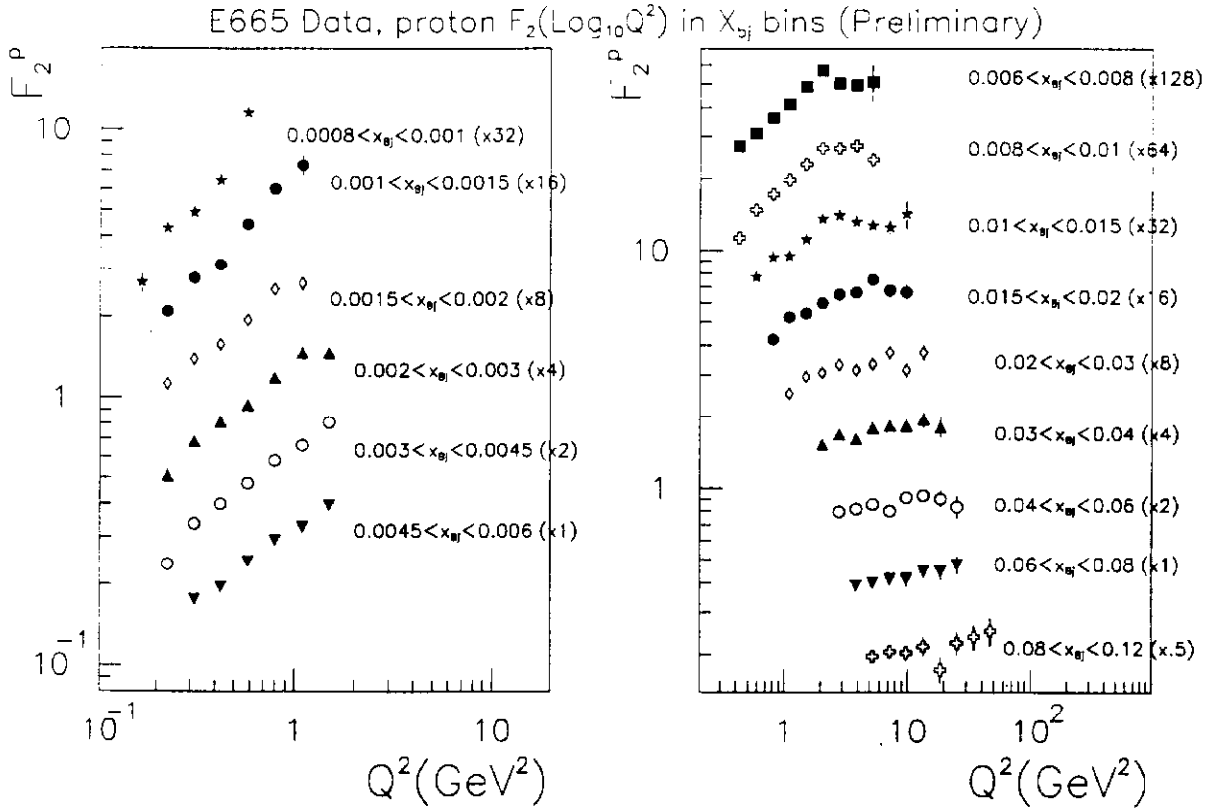

Figure 3: Preliminary Measurement of F_2 from E665 at Fermilab. These results can be compared to measurements from other charged lepton scattering experiments. For comparison to neutrino results, as in figure 1, corrections must be applied (see text).

It is extraordinarily unlikely that the discrepancy is caused by an inaccurate measurement of the strange sea, although this was suggested in several publications.[13, 14] The CCFR measurement of the strange sea, which is to next-to-leading order and includes corrections for the charm-mass threshold, would have to be incorrect by 5σ to account for the discrepancy.

In order to fully investigate the discrepancy in the F_2 measurements, data in the low x region from more than one neutrino and one muon experiment are required. Although there are data from other experiments in the higher x bins, CCFR and NMC are the only experiments to have published measurements in the region of the observed discrepancy. However, now a preliminary measurement from E665 is available and will be discussed below. A new neutrino measurement is expected from the NuTeV experiment (E815) at Fermilab after the next fixed target run.

Recently, E665 presented F_2 measurements from hydrogen and deuterium tar-

gets which cover a wide kinematic range,[15] including the region of the discrepancy between CCFR and NMC. The structure functions are shown in figure 3. Only the statistical error is shown. The systematic errors are $\approx 10 - 20\%$, coming largely from the modeling of the acceptance and the track reconstruction efficiency, and are expected to improve. The results are complementary to the HERA data which span a similar x range but at much higher Q^2. The data are in agreement with the NMC result within the systematic errors, thus reinforcing the discrepancy between the muon and neutrino measurements.

2.2 Nucleon Structure as a Test of QCD

The strong interaction is the least understood of all of the Standard Model components. Although many QCD predictions have been verified qualitatively, very few precision tests have been performed. The measurements of neutrino structure functions by CCFR provide an opportunity to make tests of the predicted evolution as well as to extract a precise measurement of Λ, the QCD mass scale.[16]

Perturbative QCD can predict the evolution of the structure functions from a starting set of x-dependent distributions.[17] This can be studied using the parity violating structure function xF_3, which represents the difference between the quark and antiquark distributions within the parton model framework. The QCD evolution of xF_3 has only one free parameter, Λ, which appears in the definition of the running coupling constant $\alpha_S(Q^2, \Lambda^2)$. The QCD fit of the CCFR data is good with $\chi^2/DOF = 53.2/53$. The extracted value of $\Lambda_{\overline{MS}}$ is $210 \pm 28\, MeV$.

An equivalent way of expressing the QCD parameter is to quote a value of α_s for Q^2 equal to the squared mass of the Z (M_Z^2). In this form, the CCFR result is $\alpha_s(M_Z^2) = 0.111 \pm 0.003(exp) \pm 0.004(th)$. This is in good agreement with other measurements from deep inelastic experiments, for which the world average is $\alpha_s(M_Z^2) = 0.113 \pm 0.005$.[18] As the value of α_s is evolved from the low Q^2 measurement to M_Z^2, the errors also evolve, resulting in a measurement which is comparable to the measurements of α_s from LEP,[18] $\alpha_s(M_Z^2) = 0.122 \pm 0.006$. Note that there is a 2σ disagreement between the deep inelastic and LEP determinations.

Figure 4 compares various measurements of α_s.[19] Each point is shown at the Q^2 associated with the measurement. The solid line indicates α_s with Λ from the deep inelastic measurement while the dashed line indicates α_s with Λ preferred by

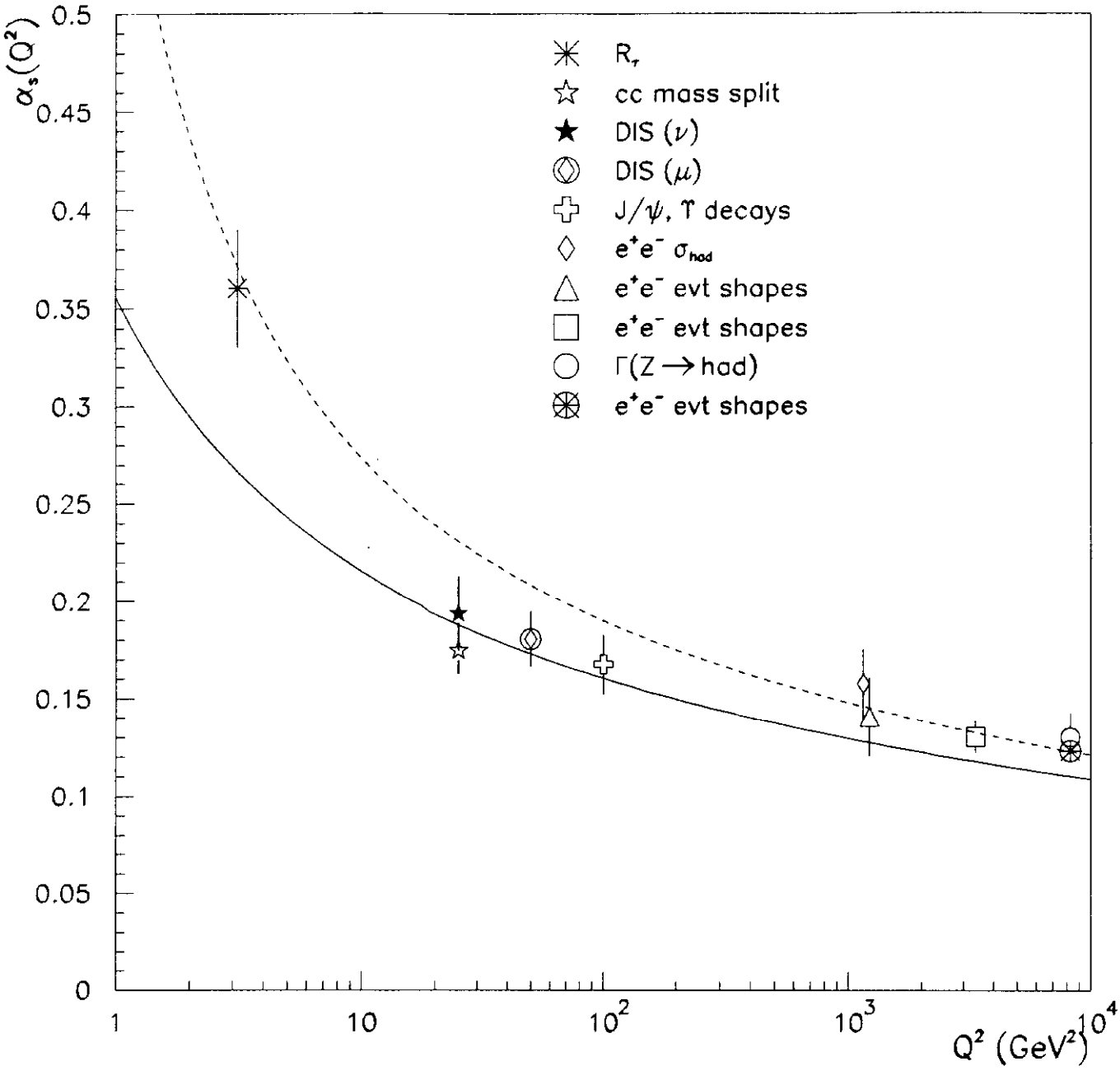

Figure 4: A compilation of measurements of α_s from various processes. The solid line indicates α_s with Λ from the deep inelastic data. The dashed curve shows α_s with Λ determined from the LEP measurements.

the LEP data. The other low-energy measurements tend to agree with the deep inelastic value for Λ. There has been significant discussion over the cause of the discrepancy between the low and high energy measurements. While some suspect a systematic problem with at least one of the measurements, others hope that this signals new physics, such as a light gluino.[20]

2.3 Measuring Individual Parton Distributions

While experiments measuring F_2 and xF_3 are sensitive to combinations of the quark and gluon distributions, other fixed target experiments at Fermilab are sensitive directly to the individual parton distributions. Two examples are Drell-Yan Experiments and Direct Photon Experiments.

The ratio of the Drell-Yan scattering cross section[21] from a target with a high neutron excess (HNE) to the scattering cross section from an isoscalar (I) target is

$$R = \frac{\sigma_{HNE}}{\sigma_I} = 1 + (\text{fractional neutron excess})\frac{\overline{d} - \overline{u}}{\overline{d} + \overline{u}}. \tag{3}$$

Thus, the ratio between the $\overline{u}$ and $\overline{d}$ seas can be extracted from a measurement of R.

Experiment E772 at Fermilab recently published results on Drell-Yan scattering from a number of heavy targets.[25] The original goals of the experiment did not include this study of the $\overline{u}$ and $\overline{d}$ sea, so unfortunately the targets were not optimized for this measurement. Data were obtained for the ratio of tungsten, which has very small fractional neutron excess of 0.183, to deuterium and carbon, which are isoscalar. No significant asymmetry in the seas was observed, but the errors were large. Much more precise data can be obtained if hydrogen is compared to deuterium, as this maximizes the fractional difference between the number of neutrons in the targets. Experiment E866, approved for the next Fermilab fixed target run, will use these targets to make a 1% measurement of the value of R at several data points in the $0.05 < x < 0.2$ region.

Measurements of the $\overline{u}$ and $\overline{d}$ seas are quite interesting because, although traditionally the u and d antiquark seas have been assumed to be equal, a recent measurement of the Gottfried Sum rule by NMC[24] indicates that $\overline{d}$ is larger than $\overline{u}$:

$$\int [(F_2^p - F_2^n)/x]\, dx = \frac{1}{3} - \frac{2}{3}\int (\overline{d} - \overline{u}) dx = 0.240 \pm 0.016. \tag{4}$$

F_2^n is extracted from measurements on deuterium which is loosely bound and may have shadowing effects. New E665 measurements of F_2^n/F_2^p in the very low x region allow investigation of shadowing in the deuteron.[22] The E665 result, $F_2^n/F_2^p = 0.94$ for $x < 10^{-2}$, is in agreement with predictions made by the model of Badelek, *et al.*,[23] which includes shadowing effects. This would translate to a 10-15% reduction to the measured value of the Gottfried Sum Rule, indicating an even larger $\bar{u}$ to $\bar{d}$ asymmetry.

Hadroproduction experiments which measure direct photon production are a second example of experiments which are sensitive to the individual parton distributions. As can be seen in figure 1, the dominant interaction which produces a direct photon directly samples the gluon distribution. There is no fragmentation function associated with the outgoing photon, making this a theoretically "clean" measurement. However, this measurement is sensitive to the definition of the QCD hard scattering variable Q^2. One way to address this problem is to search for a set of parton distributions and choice of Q^2 which simultaneously match the differential cross sections for several types of particle production. Experiment E706, which uses pion and proton beams and a beryllium target, has shown that direct photon, π^0, and η production can be described using a single set of parton distributions with the choice of $Q^2 = p_T^2/4$.[26]

3 Precision Electroweak Measurements

The Standard Model has twenty-seven free parameters. Comparison of parameters measured by a variety of methods can give hints of new physics. Although many of the parameters are measured by the fixed target experiments, this discussion will focus on $\sin^2\theta_W$ measurements from neutrino scattering and direct CP violation searches in the kaon system.

3.1 $\sin^2\theta_W$

The parameter $\sin^2\theta_W$ describes the mixing between the neutral electromagnetic field and the neutral weak field from spontaneous symmetry breaking. Unfortunately, measurements of $\sin^2\theta_W$ often also depend on the comparative strength of the neutral to charged weak couplings, parameterized by ρ. Hence, for most measurements of $\sin^2\theta_W$, the Standard Model value for ρ must be assumed. At tree

level in the Standard Model, ρ is unity. Radiative corrections, which are process-dependent, lead to small variations from unity. These radiative corrections will depend on the mass of the top quark (M_{top}) and the Higgs boson (M_{Higgs}). Various physics processes beyond the Standard Model can lead to large variations from unity. A good review of the theoretical issues involved in measuring $\sin^2\theta_W$ and ρ can be found in reference 3.

Several different types of experiments can measure $\sin^2\theta_W$. Applying the Sirlin definition,[27] $\sin^2\theta_W = 1 - (M_W/M_Z)^2$, one can use measurements of the mass of the W boson, M_W, and the mass of the Z boson, M_Z. Alternatively, $\sin^2\theta_W$ can be extracted directly from measurements of M_Z, given the Fermi coupling constant G_F. A third method uses production asymmetries in e^+e^- scattering, which are functions of $\sin^2\theta_W$. Finally, the ratio of charged-to-neutral current deep inelastic neutrino scattering events depends on $\sin^2\theta_W$. All of these measurements must assume the Standard Model dependence for ρ, except for the Sirlin definition, which has no ρ dependence by definition. Limits can be set on M_{top} and M_{Higgs}, if cross-comparisons among the above experimental measurements show good agreement. Disagreement among the experiments would hint at new physics.

The result from deep inelastic neutrino scattering, recently published by CCFR,[28] is shown in figure 5a in comparison with the other measurements described above.[29, 30] The measurement labeled "M_W" refers to the Sirlin definition with M_W from CDF and UA2, and the combined M_Z from the four LEP experiments. The "M_Z" measurement uses M_Z from LEP and G_F as input. The data points are extracted from the SLAC forward-backward and LEP left-right asymmetry measurements, respectively. One-sigma errors are presented.

The functional behavior of $\sin^2\theta_W$ *vs.* ρ within the Standard Model differs for each of the above processes. The CCFR result sweeps out a region in $\sin^2\theta_W$-ρ space which is nearly orthogonal to the other measurements. Hence, it is important for constraining the region of overlap between experiments. Presently the results are in relatively good agreement, with $M_{top} = 166^{+17+19}_{-19-22}\ GeV$ and M_{Higgs} between 60 and 1000 GeV.[30] This can be compared to the CDF preliminary top search result: $M_{top} = 174 \pm 10^{+13}_{-12}\ GeV$.[31]

Figure 5b shows the expectation for the error on these measurements in 1997, where the central values for each measurement are the 1994 values. NuTeV is the next generation of neutrino experiments at FNAL, running in 1996, and is specifically designed to measure both $\sin^2\theta_W$ and ρ. Hence instead of a broad

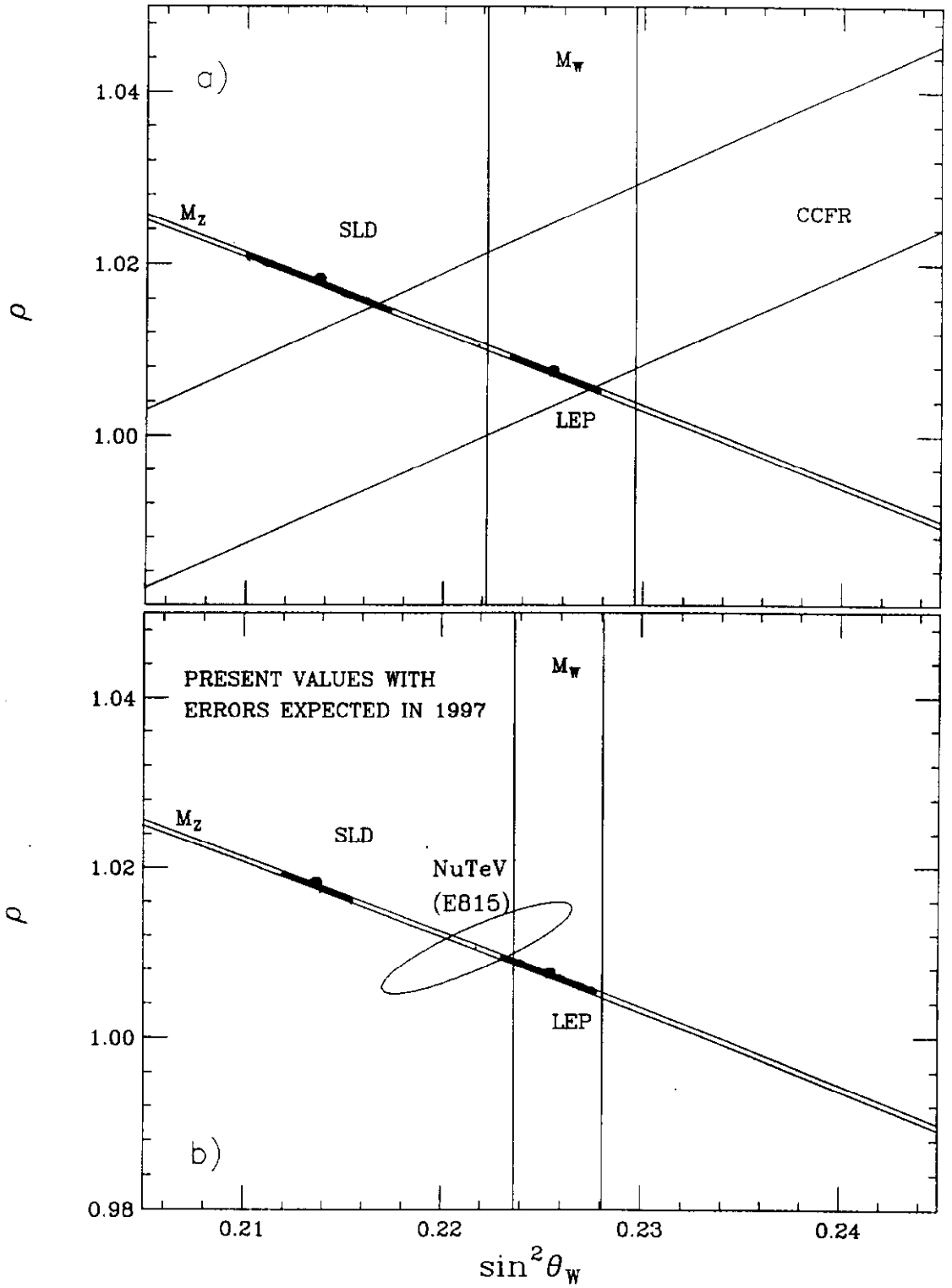

Figure 5: $\sin^2\theta_W$ *vs.* ρ from various experiments. a) Present status; b) Expected errors by 1997, central values are unchanged. The Sirlin definition of $\sin^2\theta_W$ is used.

band, this experiment will measure a small ellipse in $\sin^2\theta_W$-ρ space.[29] The improvement which will permit this measurement is a sign-selected beam, allowing separate ν and $\overline{\nu}$ measurements. By taking the ratio of neutral to charged current events in each case, one can form two equations to determine the two unknowns, $\sin^2\theta_W$ and ρ. Also, the sign-selected beam and other detector improvements are expected to reduce the systematic errors significantly.

3.2 Direct CP Violation

Evidence for CP violation has been seen in the kaon sector where experiments have observed K_L decaying to both the CP-odd (3π) and CP-even (2π) final states. In the Standard Model there are two mechanisms by which CP violation can occur. The first is mixing between CP odd and even eigenstates before decay. The second is direct decay of a particle in one CP eigenstate to a set of particles in the opposite CP state. In kaon decays, violation due to mixing is parameterized by ϵ and direct CP violation is parameterized by ϵ'. The Standard Model does permit direct CP violation to occur very rarely ($\epsilon' \ll 1$). The Superweak Model excludes direct CP violation altogether by introducing a new interaction to explain the CP asymmetry in K^0-$\overline{K^0}$ mixing ($\epsilon' = 0$).

Although most investigations of CP violation have focussed on the kaon system, there are many decay modes in which direct CP violation might be expected in the Standard Model. In the next fixed target run, the first experiment to investigate direct CP violation in the hyperon system (E871) will probe the Ξ^- and Λ^0 by comparing the decay asymmetries of the particles to the corresponding antiparticles.[32] CP violation in the D^0 system is being being explored by the charm experiments.[33] Direct CP violation in the B system is the "holy grail" of many proposed fixed target and collider experiments of all genres. However, the most stringent limits on direct CP violation have been set by kaon decay experiments and this discussion will focus on the recent kaon results from FNAL.

The "Catch-22" of CP violation in the kaon system is that ϵ'/ϵ is quite small for more common decays, while decays for which ϵ'/ϵ is expected to be large are very rare. For the relatively copious $K_L \to 2\pi$ decays, $\epsilon' \ll \epsilon$, making extraction of ϵ'/ϵ very difficult. For the rare $K_L \to \pi^0\ell^+\ell^-$ decays, $\epsilon' \approx \epsilon$. For the rare and experimentally challenging $K_L \to \pi^0\nu\overline{\nu}$, $\epsilon' \gg \epsilon$.

Experiment E731 used the $K_S, K_L \to 2\pi$ decay modes to set limits on $\Re e(\epsilon'/\epsilon)$.

According to the Standard Model, given a very massive top quark, this parameter is expected to be $\sim 10^{-3}$. The results from E731[34] are $7.4 \pm 5.2\,(stat) \pm 2.9\,(sys) \times 10^{-4}$ which is consistent with zero. This can be compared to the results from NA31,[35] a similar experiment at CERN, which measured $23 \pm 6.5 \times 10^{-4}$, more than 3σ away from zero. In the next fixed target run, KTeV is expected to reduce the errors on this measurement by a factor of five.

Alternatively, one can look to rare decays for evidence of direct CP violation. Among the many decays studied by E799 at FNAL, the three "cleanest" modes theoretically are $K_L \to \pi^0 e^+ e^-$, $K_L \to \pi^0 \mu^+ \mu^-$, and $K_L \to \pi^0 \nu \bar{\nu}$. The Standard Model predicts CP violation at the 10^{-11} level for the first two decays and at the 10^{-10} level in the third channel. The decays in the electron and muon modes were ruled out by E799 at the 4.3×10^{-9} and 5.1×10^{-9} levels respectively.[36, 37] The third channel is experimentally very difficult to observe and the E799 limit[38] of 5.7×10^{-5} represents an important proof-of-principle for searching in this mode in future running periods.

Increasingly larger samples of K_L decays are expected in the next fixed target run and the runs following the main injector upgrade. This will lead to very sensitive limits on direct CP violation in these rare decays, or perhaps a discovery!

4 Heavy Quark Studies

Studies of heavy meson production can address questions in both QCD and the electroweak framework. Within perturbative QCD, calculations for bound states and for production of massive quarks are more straight-forward than for lighter quarks because perturbative techniques can be applied. Therefore production of c- and b-mesons can provide meaningful tests of QCD. The studies of heavy meson lifetimes and fragmentation can address issues of final state interactions. Intrinsic heavy quark distributions can be measured.[39] Measurements of branching ratios allow extraction of the CKM matrix parameters. Searches provide limits on rare decays and therefore on new physics.

The experiments at Fermilab have amassed samples of more than 10^5 charmed meson and baryon decays. The most recent experiments to publish results are E653, E760, E687 and E769/791. In the 1996 fixed target run, E831 expects a charm meson yield of $\sim 10^6$. The first experiment to study high-x charm baryon production, E781 (Selex), will take data in the next running period. The

charmonium program (E835) also will continue.

This review will cover new observations of charmed baryons and mesons and new results on charm fragmentation. Recently announced measurements of lifetimes and widths, energy dependence of the charm cross section, CKM matrix elements, and D^0–$\overline{D^0}$ mixing will not be covered here.[40]

The study of b-mesons in a fixed target setting is in its infancy. In principle a fixed target experiment has several advantages: a very forward boost leading to well-separated secondary vertices, a large acceptance for particle identification detectors, and the opportunity to use high-A targets. In practice, this study is extremely difficult because the rates at present fixed target energies are low. FNAL E653 and E672/E706 have presented results on the b cross-section as a function of momentum.[41, 42] Recently E789 has presented preliminary results on the differential cross section as a function of p_T.[43] These results were presented at this Topical Conference by W. Yao, "CDF Evidence for the top and B physics at Fermilab," and will not be discussed here.

4.1 Mysteries of the Missing Charm

Several theoretically expected charm states are poorly-observed or unobserved. This discussion covers the Ω_c^0 baryon, which has now been observed by E687, and several charmonium states under study by E760.

Evidence for the elusive Ω_c^0 has now been published by three experiments. WA62 at CERN reported three events in the channel $\Xi^- K^- \pi^+ \pi^+$ at $2740 \pm 20\ MeV$.[44] Argus announced a signal from 12.2 ± 4.5 events in the same channel at $2719 \pm 8\ MeV$.[45] Now E687 at Fermilab has reported signals in two channels:[46, 47] $\Omega^- \pi^+$ and $\Sigma^+ K^- K^- \pi^+$ where the Σ^+ decays to $p\pi^0$ or $n\pi^+$. From 10.3 ± 3.9 events, E687 measured a mass of $2705.9 \pm 3.3 \pm 2.0\ MeV$ in the first channel. In the second channel, the mass was measured to be $2699.9 \pm 1.5 \pm 2.5\ MeV$ from 42.5 ± 8.8 events. This is the strongest published evidence for the Ω_c^0 to date. Although E687 has not published a combined fit for the two channels, it is reasonable to take the statistically weighted average of the two measurements and assume the systematics are the same, giving $2700.9 \pm 1.4 \pm 2.5\ MeV$ as the mass of the Ω_c^0.

Several charmonium states are also "missing-in-action." The properties of charmonium are particularly interesting because charmonium can be regarded as

Resonance	Mass (MeV)	Width (keV)
J/ψ (E-760)	$3096.88 \pm 0.01 \pm 0.06$	$99 \pm 12 \pm 6$
J/ψ (Old Value)	3096.93 ± 0.09	86 ± 6
χ_1 (E-760)	$3510.53 \pm 0.04 \pm 0.12$	$880 \pm 110 \pm 80$
χ_1 (Old Value)	3510.6 ± 0.5	< 1300
χ_2 (E-760)	$3556.15 \pm 0.07 \pm 0.12$	$1980 \pm 170 \pm 70$
χ_2 (Old Value)	3556.3 ± 0.4	$2600\ ^{+1200}_{-900}$
$\chi_2 - \chi_1$ (E-760)	$45.62 \pm 0.08 \pm 0.12$	
ψ' (E-760)	3686.0 (input)	$312 \pm 36 \pm 12$
ψ' (Old Value)	3686.0 ± 0.1	243 ± 43

Table 1: Summary of new results on resonance parameters from E760 compared to previous results. See reference 49.

the "positronium" of QCD, allowing very precise tests of predictions. In the last series of runs, E760 took $p\bar{p}$ data using an apparatus located in the anti-proton accumulator ring of the collider. This experiment observed the $^1P_1$ charmonium state for the first time.[48] The η_c and η_c' are presently under study. As shown in table 1, the new FNAL results provide precise measurements for the masses and widths of the χ and ψ states.[49]

E835, which will take data in the next fixed target run, will continue these charmonium studies.[50] This experiment plans to measure the mass and total width of the η_c' and its decay to $\gamma\gamma$, to improve the measurements of the η_c parameters and to continue studies of the $^1P_1$ state. It also will focus on a search for another set of missing charmonium mesons: the $^{3,1}D_2$ states.

4.2 Production Asymmetry for $D^{\pm}$ Mesons

The production asymmetry between leading and non-leading D mesons is measured in hadroproduction experiments such as E769 and E791. E769 used a tagged-beam system, taking the asymmetry data presented below with both π^- and π^+ beams. E791 has two orders of magnitude more statistics, but used only a π^- beam.

A meson with $x_F > 0$ that has a light quark in common with the incoming beam particle is referred to as a "leading particle." For example, for π^- $(\bar{u}d)$ scattering, forward D^- $(\bar{c}d)$ mesons are leading and D^+ $(c\bar{d})$ are non-leading. The asymmetry is defined as:

$$A = \frac{N_l - N_n}{N_l + N_n} \tag{5}$$

where N_l and N_n are the numbers of leading and non-leading D mesons respectively.

Several sources for such an asymmetry are possible. Next-to-leading-order QCD calculations predict a small asymmetry for π^- scattering.[51] Alternatively, in the Intrinsic Charm Model,[52] the incoming pion can fluctuate into a state with a virtual $c\bar{c}$ which may be knocked onto the mass shell. When the $\bar{c}$ combines with the d valence quark of the π^-, a very high x_F leading D^- is produced. Finally, some fragmentation models, such as the Lund/Pythia model,[53] add momentum to the charmed quark if it combines with a valence quark, phenomenologically reproducing the asymmetry. In each of these processes, the expected behavior of the asymmetry as a function of x_F and p_T^2 differ.

Figure 6 shows the measured asymmetries from E769 and E791 as functions of x_F and p_T^2.[54, 55] Only approximately half of the E791 data were used in this analysis. Data from the WA82 experiment at CERN are also shown.[56] The corresponding predictions from QCD, Pythia and Intrinsic Charm Models are indicated. The QCD prediction underestimates the effect. The data lie between the Pythia and Intrinsic Charm models and in some regions are inconsistent with both predictions. The asymmetry is confirmed but its source is still unclear. The high statistics and doubly differential distributions from E791 may provide additional guidance.

5 Polarization and Magnetic Moment Measurements

An interesting feature of high energy collisions is that an unpolarized beam scattering from an unpolarized target can result in production of polarized particles. The cause of this polarization remains a mystery. Polarization is most striking in the hyperon family where the effects can be quite large. Fermilab has had an

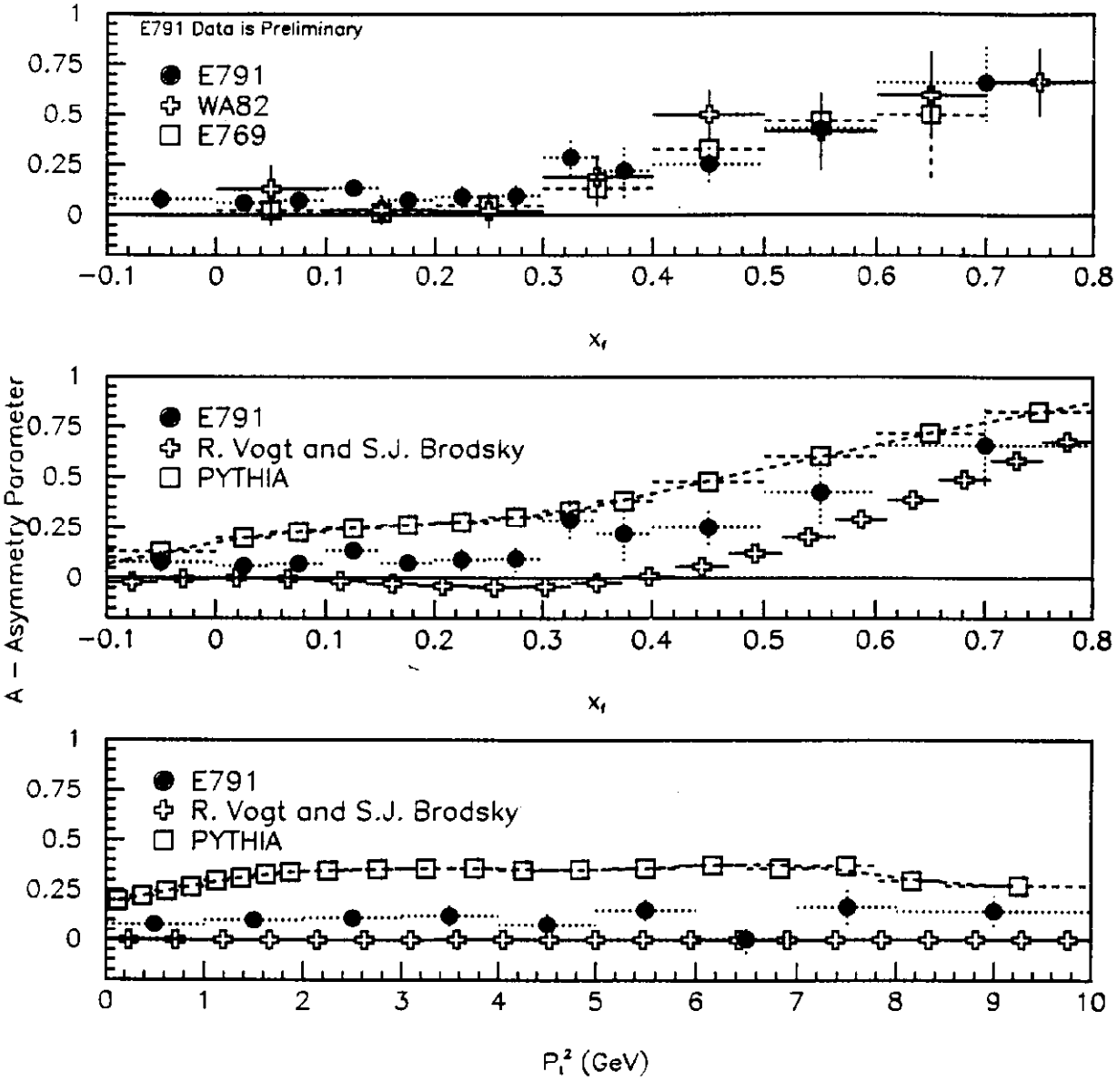

Figure 6: The asymmetry in D meson production from E769 and E791 at FNAL and WA82 at CERN are shown as a function of x_F and p_T^2. Predictions for the Intrinsic Charm Model (Vogt and Brodsky) and PYTHIA (Sjostrand) are shown.

extensive program of hyperon experiments which exploit and measure these polarization effects. In particular, polarization allows magnetic moment measurements through spin precession in a magnetic field. The 1994 APS Panofsky Prize was given to Thomas J. Devlin and Lee G. Pondrom for hyperon studies at FNAL.

5.1 Polarization of Hyperons

Polarization has been measured for all of the hyperon family by a series of FNAL experiments. Each apparent pattern for the magnitude or sign of the polarization as a function of p_T, x_F or energy has unexplainable exceptions. For example, E799 recently showed that the Λ^0 polarization depends on p_T, but has no energy dependence[59] while E761 has shown that the Σ^+ and the Ξ^- have energy dependences to their polarization which show opposite trends.[60] Figure 7 compares the polarizations of the Σ^+, Λ^0 and the Ξ^- as functions of x_F and p_T. The behaviors are quite different for the three particles.

5.2 Magnetic Moment Measurements

Almost two decades of work has led to very precise measurements of the magnetic moments of the hyperons. The most recent measurements from the FNAL program are on the Σ from E761.[62] A new measurement from E800 on the magnetic moment of the Ω^- is expected soon.

In principle, the "simple quark model" predicts the moments for Σ, Ξ, Ω and Δ given the measured moments of the proton, neutron and Λ.[61] In practice, there are large deviations from the predictions which must be attributed to low energy effects. More sophisticated models such as the lattice calculations, the Skyrme model, the Bethe-Salpeter formalism, and the relativistic quark model have been suggested.

Among the choices for models, the relativistic quark model[63] is quite good. It is simple and describes the data,[64] as shown in table 2. This calculation, which uses light cone variables, is straightforward. The parameters of this model are the constituent quark mass, the "size" of the baryon, and the choice of wavefunction. The best fit uses a symmetric wavefunction.

It may be possible to study magnetic moments in the charm baryon systems in the next generation of accelerators.[57] If charm baryons are produced at energies $\sim 1\,TeV$, the decay length is $\sim 4\,cm$. The baryon can be directed through a bent

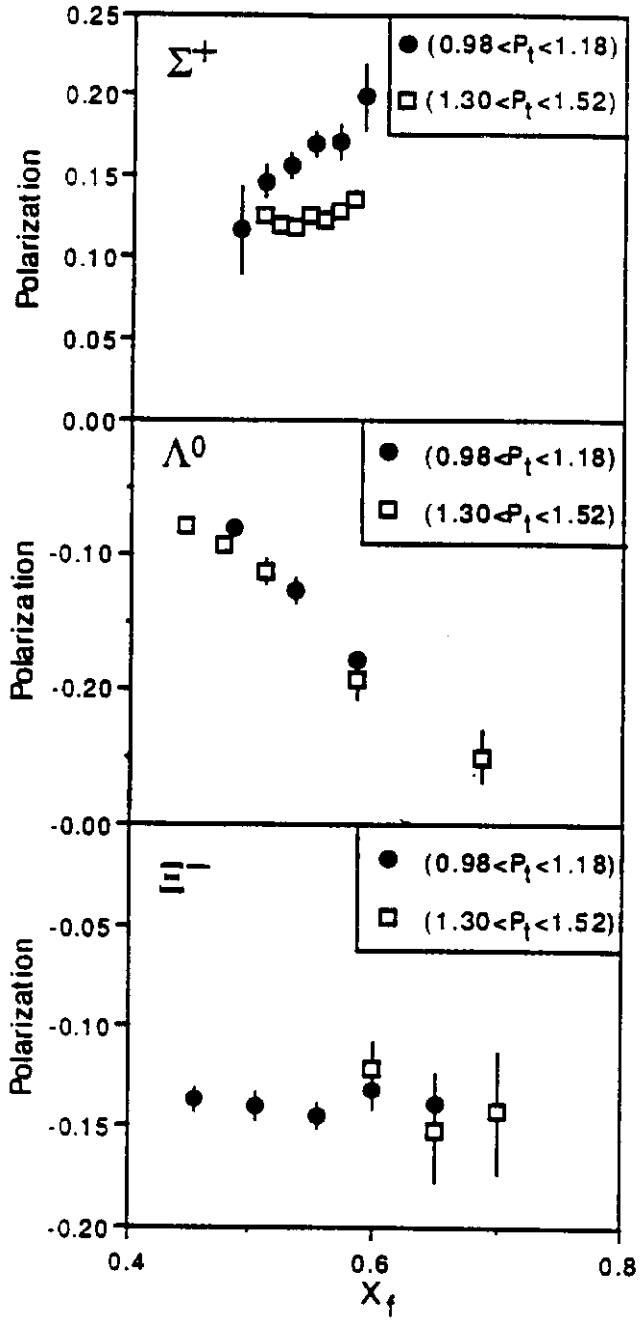

Figure 7: Comparison of the polarization of the Σ^+, Λ^0 and Ξ^- as functions of x_F for two regions of p_T from E761.

Particle	Expt. Magnetic Moment (from ref. 64)	Model Fit Value (from ref. 63)
Σ^+	2.42 ± 0.05	2.55
Σ^-	-1.160 ± 0.025	-1.07
Λ	-0.613 ± 0.004	-0.61
Ξ^0	-1.250 ± 0.014	-1.33
Ξ^-	0.6507 ± 0.0025	-0.68

Table 2: Comparison of experimental measurements of the hyperon magnetic moments to the fits from the relativistic quark model.

crystal lattice with large effective magnetic fields. Implanted silicon detectors can be used to measure the track. The magnetic moment of the Σ^+ has been measured using crystal channeling as a demonstration of this method.[58]

6 Searches for New Phenomena

The fixed target experiments provide many opportunities to search for new phenomena even though these experiments are not at the high energy frontier. Searches are performed through precision measurements of electroweak parameters as discussed above and through direct searches for processes unpredicted or forbidden by the Standard Model.

This discussion will focus on experimental tests for neutrino oscillations, however, other searches deserve comment. Limits on forbidden π^0 and K_L decays have been published this year by the E799. For example, $\pi^0 \rightarrow \mu^{\pm} e^{\mp}$, which is a lepton number violating process, has been ruled out to the level of 8.6×10^{-9}.[65] Also, the neutrino experiments recently have set limits for leptoquark and neutral heavy lepton production.[66]

Neutrino oscillations refer to transitions between the neutrino species, $\nu_e \leftrightarrow \nu_\mu$, $\nu_\mu \leftrightarrow \nu_\tau$, and $\nu_e \leftrightarrow \nu_\tau$, in analogy with flavor mixing in the quark sector. The oscillation between two neutrino species is described by two parameters: α, which represents the mixing between the mass eigenstates and the species eigenstates, and $\Delta m^2 = m^2_{\nu 2} - m^2_{\nu 1}$, which is the squared mass difference between the two

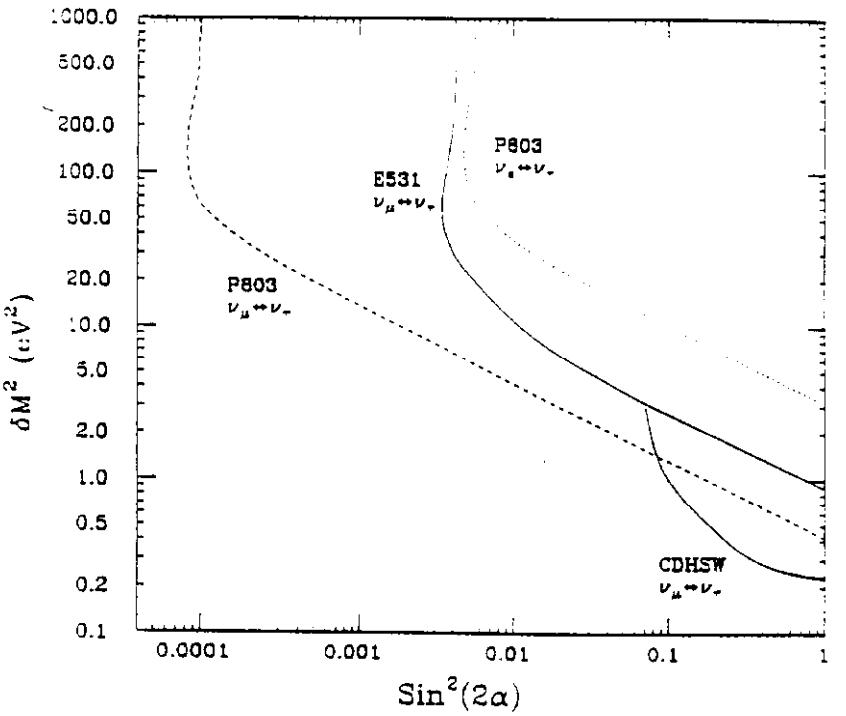

Figure 8: Limits on Neutrino Oscillations from Short Baseline Detectors. Present limits are indicated by solid line. Dashed line shows E803 sensitivity.

species. The probability of oscillation is given by

$$P(\nu_1 \rightarrow \nu_2) = \sin^2 2\alpha \ \sin^2(1.27\Delta m^2 \frac{L}{E}) \tag{6}$$

where L is the path length from production to detection of the neutrinos in kilometers and E is the neutrino energy in GeV.

For large values of Δm^2, equation 6 reduces to $\frac{1}{2}\sin^2 2\alpha$. Hence, experiments with neutrino beams of small path length ("short baseline") can still be sensitive to oscillations with small mixing angles. Large L ("long baseline") experiments are sensitive to the term containing Δm^2, even for small mass differences.

Massive neutrinos have been invoked to explain various mysteries including the closure of the universe, the atmospheric neutrino deficit, and the solar neutrino problem.[6, 67] A theoretical prejudice of astrophysics is that the mean density of the universe is equal to the critical density, thereby "closing" the universe. If so, then 90% of the matter is "dark" as opposed to "visible." Neutrinos with small masses could account for some of the dark matter. The atmospheric neutrino deficit refers to the observation of fewer than expected muon neutrinos from cosmic-ray proton

interactions in the atmosphere. Oscillations of $\nu_\mu \leftrightarrow \nu_\tau$ could explain the deficit. Finally, the solar neutrino problem, the apparent deficit of ν_e's from the sun, could also be explained by oscillations.

Portions of the regions in Δm^2-$\sin^2 2\alpha$ space which are of interest for the cosmological and atmospheric neutrino questions are accessible to accelerator experiments if very large samples of neutrinos can be acquired. The upgraded Main Injector will produce 3×10^{13} protons every 1.9 seconds, resulting in the most intense neutrino beam ever created. Hence Fermilab is an ideal place to base these studies.[6]

6.1 The Short Baseline Program

E803, the short-baseline experiment, will search for the appearance of ν_τ's in a beam of ν_μ's.[68] The neutrino beam will travel approximately $1\,km$ before hitting an emulsion target. The experiment searches for the charged-current interaction $\nu_\tau + h \rightarrow \tau + X$ in the emulsion by observing the kink in the tracks from the τ decay. The design of E803 is similar to its predecessor, E531,[69] and its competitor CHORUS at CERN.[70] An emulsion target is followed by tracking chambers in a magnetic field for precise momentum measurements. A series of chambers following a hadron absorber allows muon detection. The technique of detecting ν_τ events in emulsion will be tested in the next fixed target run by the beam-dump experiment E872.[71] This experiment may provide the first observation of ν_τ interactions.

The short baseline makes E803 sensitive to low values of $\sin^2 2\alpha$ but not low values of Δm^2. The proposed range for E803 is shown in figure 8. Recent improvements in scanning technology may permit even better sensitivity for E803. This is compared to the limits from E531 and to results from CDHSW, a neutrino deep inelastic scattering experiment which took data at CERN in 1983.[72] CHORUS is expected to set limits which are approximately an order of magnitude better than E531 and an order of magnitude less than E803.

6.2 The Long Baseline Program

A long-baseline experiment would be sensitive to the region of $\sin^2 2\alpha$-Δm^2 space where the atmospheric neutrino deficit has piqued interest. If one interprets the observed deficit[73] as a signal for oscillation, then the most probable values for the

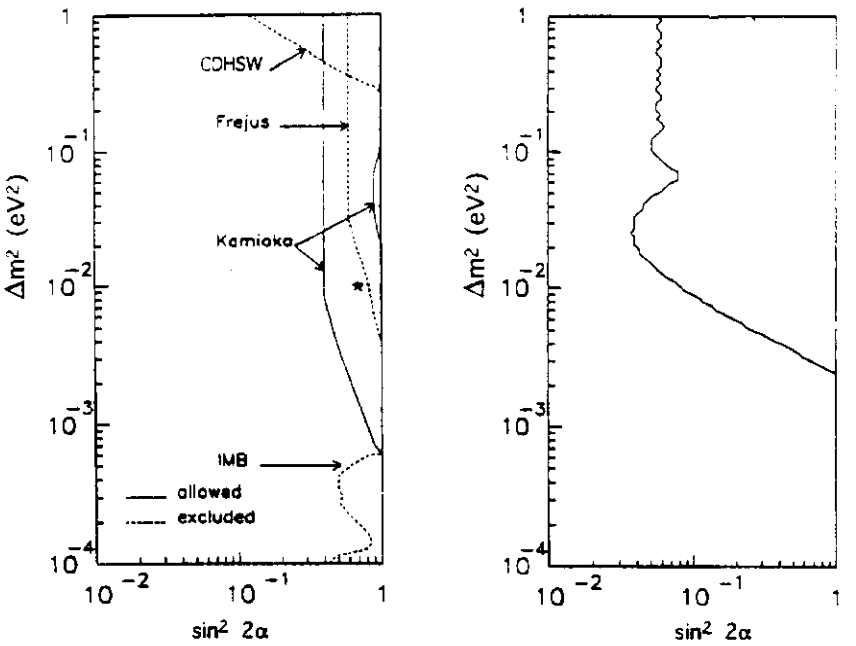

Figure 9: Limits on Neutrino Oscillations from Long Baseline Detectors. a) Solid line shows allowed region, $\star$ is "best value", dashed line shows excluded region. b) Expectations for the Soudan 2 detector.

parameters are $\Delta m^2 \approx 10^{-2}$ and $\sin^2 2\alpha \approx 0.69$.[6] Figure 9a indicates the allowed region by the solid lines. The dashed lines indicate regions which have been ruled out by various experiments.[72, 74]

Although a long baseline program has been approved at Fermilab, neither the site nor the design of the experiment has been determined. As a result, the exact regions which will be probed in $\sin^2 2\alpha$ and Δm^2 space have not been determined. The far detector is expected to be at least 100 *km* from the FNAL site and to have a mass of more than 10 kilotons. Options which have been presented include using the Soudan (Minnesota), Dumand (Hawaii) and IMB (Ohio) sites.[75] Figure 9b indicates the limit expected from the Soudan 2 detector.

A long-baseline detector allows both appearance and disappearance experiments. The appearance experiment would be designed to look for ν_τ interactions. The disappearance experiment would look for an unexpected reduction in the ν_μ flux. A disappearance experiment uses two detectors: one with a short baseline which measures the original flux and one with a long baseline which measures the final flux. After corrections, a difference in flux measurements would indicate oscillations. One clever idea which reduces systematic errors on the corrections is to measure the ratio of neutral- to charged-current interactions in the near and

far detectors rather than relying on absolute flux measurements.[76]

7 Conclusions

The purpose of this discussion is to give the reader a flavor of the Fermilab Fixed Target Program. The program is thriving, with the following impact:

- Some of the fixed target results are competitive with measurements from the collider or from other laboratories. Disagreements between measurements of almost equal accuracy of the same parameters, as in ϵ'/ϵ, emphasize the need for further exploration.
- Some of the results are complementary to the collider and other programs. One example among many is the hadron structure measurements, which, used in conjunction with results from the Fermilab collider and from HERA, provide the foundation for our understanding of the parton distributions.
- Some of the results are unique. For example, the NuTeV neutrino experiment, which will run in 1996, will provide the only direct measurement of the parameter ρ, which is sensitive to many sources of new physics.
- All of the results are timely and exciting.

The breadth and depth of the FNAL program make it unique among the fixed target programs at the various HEP laboratories. The experiments address important topics. Within each topic, several experiments attack the issues from various viewpoints. In the upcoming run, this program continues in the same spirit, with experiments that continue to address the issues outlined here. The Main Injector Upgrade will herald a renaissance of fixed target experiments at Fermilab, probing the most fundamental issues of our field.

Thanks

Many people contributed to this review, particularly Bob Bernstein, Tom Carter, Harry Cheung, Debbie Harris, Joe Lach, Kevin McFarland and Stephen Pordes. The Fermilab Program is supported by the U.S. Department of Energy. The National Science Foundation contributes funding for many of the experiments.

References

[1] The fixed target program published forty-four papers during this period in *Physical Review D, Physical Review Letters, Physics Letters B,* and *Zeitshcrift für Physik* alone. A list, compiled by Peter Garbincius, of all FNAL of publications during the last fiscal year which appeared in these four journals is available from Peter Garbincius (garbincius@fnalv.fnal.gov), MS 122, PO Box 500, Batavia, Il 60510.

[2] Sterman, *et al.*, Handbook of Perturbative QCD, Fermilab-Pub-93/094, April 1993, accepted for publication in Reviews of Modern Physics. It describes the basic ideas of hadron structure measurements and perturbative QCD.

[3] Langacker, UPR-0594-T, 1994, to appear in the proceedings of the INS International Symposium on Physics with High Energy Colliders, Tokyo, 8-10 March 1994. Covers the present status the Standard Model in light of recent precision electroweak measurements and the probable discovery of the top quark by CDF.

[4] Buras and Linder, Heavy Flavors, World Scientific (1993). This is a good review book on heavy flavor physics.

[5] Lach, Fermilab-Conf-94/031 (1994). Cooper, Fermilab-Conf-93/403-E. These articles cover physics of radiative decays, polarization and magnetic moments in the hyperon system. Both will be published in the proceedings of The U.S./Japan Seminar: The Hyperon-Nucleon Interaction, Maui (1993).

[6] Bernstein, *et al.*, Neutrino Physics After the Main Injector Upgrade, Fermilab Conceptual Design Report, 1994. Available upon request from the FNAL library. It describes the physics motivation and experimental goals of the FNAL ν oscillation experimental program.

[7] The Fermilab Workbook is available through Fermilab Program Planning, PO Box 500, Batavia, Il 60510.

[8] Bazarko, *et al.*, Nevis-1502, (1994). Submitted to Z. Phys. C.

[9] Amaudruz, *et al.*, Z. Phys. C51, (1991) 387.

[10] Quintas, Nevis Preprint 277, (1992).

[11] Amaudruz, *et al.*, Phys. Lett. B295 (1992) 159.

[12] Carroll, "Observation of Nuclear Shadowing at low x in Carbon, Calcium, and Lead," Thesis, University of Illinois, Urbana (1994).

[13] Botts, *et al.*, Phys. Lett. B304 (1993) 159.

[14] Barone, *et al.*, Phys. Lett. B328 (1994) 143.

[15] Kotwal, *et al.*, Fermilab-Conf-94-251 (1994), to be published in the proceedings of the 1994 Meeting of the American Physical Society, Division of Particles and Fields, Albuquerque 2-6 Aug (1994).

[16] Quintas, *et al.*, A Measurement of $\Lambda_{\overline{MS}}$ from ν_μ Fe structure functions at the Tevatron. Phys. Rev. Let., 71, 1307 (1993).

[17] Altarelli, *et al.*, Nucl. Phys. B126 (1977) 298.

[18] Virchaux, QCD: 20 Years Later (Proceedings of the workshop at Aachen, Germany, June 9-13, 1992), World Scientific Publishing, (1993) 205.

[19] Hinchliffe, Phys Rev D:50 (1994) 1297.

[20] Blumlein, *et al.*, Phys. Lett. B325 (1994) 190.

[21] Drell, *et al.*, Phys. Rev. D:1 (1970) 2402.

[22] Spentzouris, *et al.*, Fermilab-Conf-94-220-E (1994), to be published in the proceedings of the Intersections of Particle and Nuclear Physics, St. Petersburg, FL, 31 May - 6 June, (1994).

[23] Badelek, *et al.* , Phys. Rev. D50 (1994) 4.

[24] Amaudruz, *et al.*, Phys. Rev. Lett. 66 (1991) 2712.

[25] McGaughey, *et al.*, Phys. Rev. Lett 69 (1992) 1726.

[26] Alverson, *et al.*, Phys. Rev. D48 (1993) 5.

[27] Sirlin, Phys. Rev. D:22 (1980) 971.

[28] King, *et al.*, Phys. Rev. Lett., 72 (1994) 3452.

[29] Shaevitz, *et al.*, to be submitted to the proceedings of Neutrino '94, Eilat, 30 May - 3 June (1994).

[30] Uses weighted average of the UA2 and CDF M_W measurements: Alitti, *et al.*, Phys. Lett. B276 (1992) 354; Abe, *et al.*, Phys. Rev. D43 (1991) 2070; The LEP Collaborations, Phys. Lett. 307B (1993) 187.

[31] Abe, *et al.*, Phys. Rev. D50 (1994) 2966. Abe, *et al.*, Phys. Rev. Lett. 73 (1994) 225.

[32] Luk, *et al*, Fermilab-Proposal-P-871 (1993).

[33] Frabetti, *et al.*, Phys. Rev. D50 (1994) R2953.

[34] Gibbons, *et al.*, Phys. Rev. Lett, 70 (1993) 1203.

[35] Barr, *et al.*, Phys. Lett. B317 (1993) 233.

[36] Harris, *et al.*, Phys. Rev. Lett, 71 (1993) 3914.

[37] Harris, *et al.*, Phys Rev Lett, 71 (1993), 3918.

[38] Weaver, *et al.*, Phys Rev Lett 72 (1994) 3758.

[39] Combridge, Nucl. Phys. B151 (1979) 429. Brodsky, *et al.*, Phys. Lett. 93B (1980) 451.

[40] New measurements include: Frabetti, *et al.*, Phys. Rev. Lett. 71 (1993) 827; Kodama, *et al.*, Phys. Lett. B336 (1994) 605; Frabetti, *et al.*, Phys. Lett. B323 (1994) 459; Frabetti, *et. al.*, Phys. Lett. B328 (1994) 187; Frabetti, . *et al.*, Phys. Lett. B328 (1994) 193; Frabetti, . *et al.*, Phys. Rev. Lett. 72 (1994) 961.

[41] Kodama, *et al.*, Phys. Lett. B303 (1993) 359.

[42] Jesik, *et al.*, Fermilab-Pub-94-095-E (1994), submitted to Phys. Rev. Lett.

[43] Jansen, *et al.*, FERMILAB-CONF-93-129-E (1993).

[44] Biagi, *et al.*, Z. Phys. C28 (1985) 175.

[45] Albrecht, *et al.*, Phys Lett B288 (1992) 367.

[46] Frabetti, *et al.*, Phys. Lett. B300 (1993) 190.

[47] Frabetti, *et al.*, Phys. Lett. B338 (1994) 106.

[48] Armstrong, *et al.*, Phys. Rev. Lett., 69 (1992) 2337.

[49] Hasen, *et al.*, Nucl. Phys. A558 (1993) 53. Pordes, *et al.*, Fermilab-Conf-93-383 (1993), submitted to the proceedings of The Advanced Studies Conference on Heavy Flavours, Pavia, 3-7 September (1993).

[50] Armstrong, *et al.*, Fermilab-Proposal-P-835 (1993).

[51] Nason, *et al.*., Nucl. Phys. B372, (1989) 49.

[52] Vogt, *et al.*, SLAC-PUB-6468 (1994).

[53] Sjostrand, CERN-TH 6488/92 (Pythia 5.6 Manual) (1992).

[54] Alves, *et al.*, Phys. Rev. Lett., 72 (1994) 812. Also see Erratum, Phys. Rev. Lett., 72 (1994) 1946.

[55] Carter, to be published in the proceedings of the 1994 Meeting of the American Physical Society, Division of Particles and Fields, Albuquerque 2-6 Aug (1994).

[56] Adamovich, *et al.*, Phys. Lett. B305 (1993) 402.

[57] Carrigan, *et al.*, Proceedings of The Future of High-Sensitivity Charm Experiments: Proceedings of the CHARM2000 Workshop, Batavia 7-9 June (1994) 123.

[58] Chen, *et al.* , Phys. Rev. Lett., 69 (1992) 3286.

[59] Ramberg, *et al.*, Fermilab-Pub-94-015 (1994), submitted to Phys. Rev. Lett.

[60] Morelos, *et al.*, Phys. Rev. Lett. 71 (1993) 3417.

[61] A good discussion of predictions from the simple quark model for can be found in Close, An Introduction to Quarks and Partons, Academic Press, (1979).

[62] Morelos, *et al.*, Phys. Rev. Lett. 71 (1993) 3417.

[63] Schlumpf, Phys. Rev. D:47 (1993), 4114. Also see Erratum, Phys. Rev. D:49 (1994) 6246.

[64] From Baryon Listings, Particle Data Group, Phys Rev D:50, 1673.

[65] Krolak, *et al.*., Phys. Lett. B:320 (1994) 407.

[66] Lefmann, Thesis and Nevis Preprint in preparation.

[67] Perkins, Nucl. Phys. B399 (1993) 3.

[68] Kodama, *et al.*, Fermilab-Proposal-P-803 (1993).

[69] Ushida, *et al.*, Phys. Rev. Lett. 57 (1986) 2897.

[70] Buontempo, *et al.*, CERN-PPE-94-19 (1994). Submitted to Nucl. Inst. Meth. Lendermann, *et al.*, Nucl. Inst. Meth. A344 (1994) 143.

[71] Lundberg, *et al.*, Fermilab-Proposal-P-872.

[72] Dydak, *et al.*, Phys. Lett. B134 (1984) 281.

[73] Hirata, *et al.*, Phys. Lett. B205 (1988) 416. Casper, *et al.*, Phys. Rev. Lett. 69 (1992) 1010.

[74] Berger, *et al.*, Phys. Lett. B245 (1990) 305.

[75] See Fermilab-Proposal-P-805 (1990) – IMB site; Fermilab-Proposal-P-822 (1991) – Soudan site; Fermilab-Proposal-P-824 (1990) – Dumand site.

[76] Bernstein, *et al.*, Phys. Rev. D44 (1991) 2069.

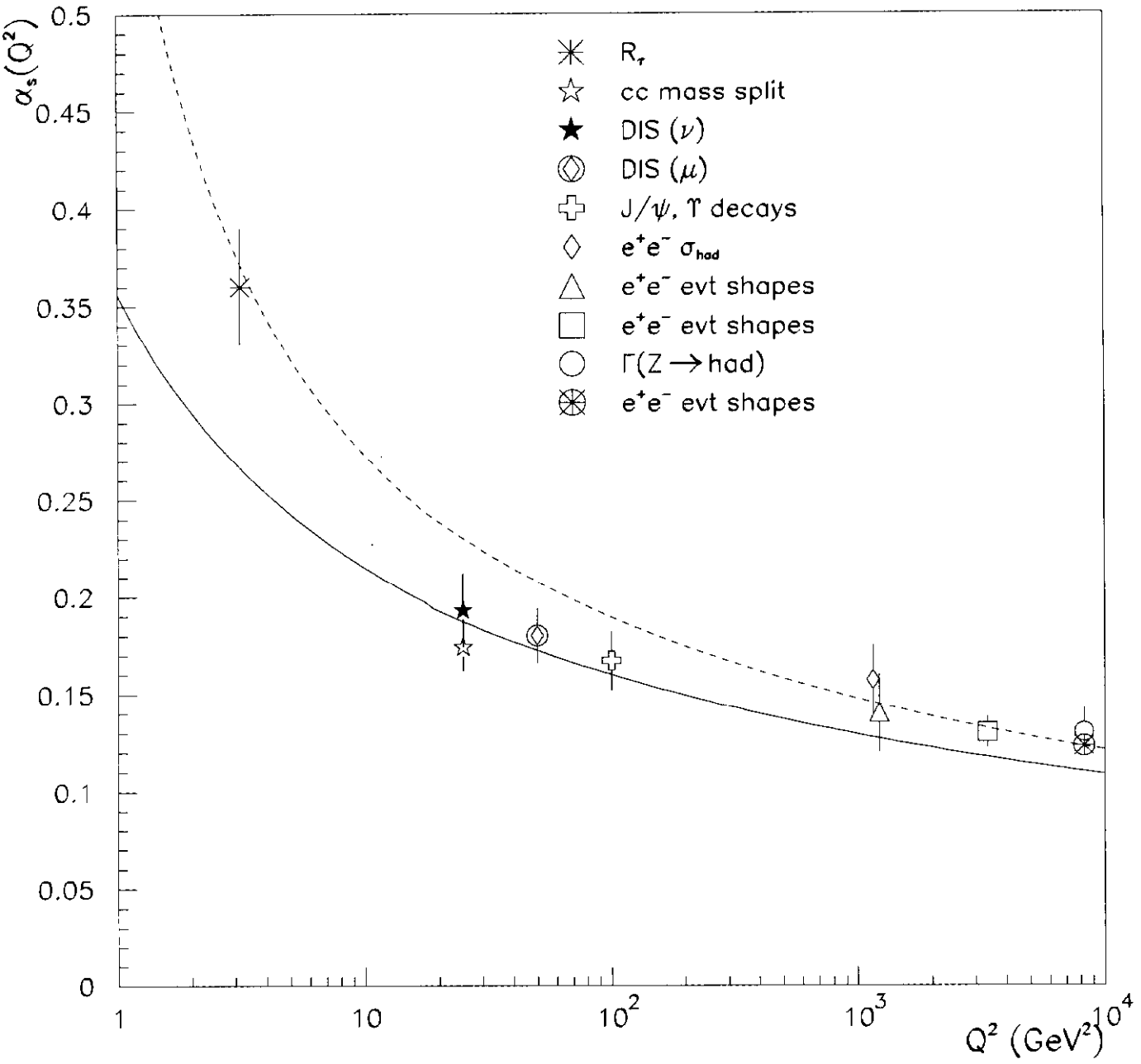

Figure 4: A compilation of measurements of α_s from various processes. The solid line indicates α_s with Λ from the deep inelastic data. The dashed curve shows α_s with Λ determined from the LEP measurements.